

# IMPACT OF DUAL TIME POINT FDG PET IMAGING IN THE ASSESSMENT OF SOLITARY PULMONARY NODULES

*Khaled Alkhaldeh MD\*, Samir Khraisat MD\*, Abass Alavi MD\*\**

## ABSTRACT

**Objective:** The aim of this study was to assess the diagnostic potential of  $^{18}\text{F}$ -FDG Positron Emission Tomography imaging in the evaluation of patients with solitary pulmonary nodules, by comparing the diagnostic criteria in single time point imaging method to two different diagnostic criteria in dual-time-point imaging.

**Methods:** This retrospective study was conducted in the Hospital of the University of Pennsylvania, and data was collected and analyzed in the period from September 2005 to March 2006, from the pooled hospital studies for the last eight years. Two hundred sixty five patients were included (161 men, 104 women, age range: 41–92 years). All had solitary pulmonary nodules on computed tomography, and the diagnosis was confirmed by biopsy or by follow up computed tomography. All 265 patients underwent whole body FDG PET scan, and 255 of them had PET scan two time points. The maximum standardized uptake values of nodules were calculated for both time points. On single time point imaging we set the maximum standardized uptake value of 2.5 as a cutoff criterion for malignancy. On dual time point imaging, first criterion of malignancy was set as any increase in the maximum SUV from the first to second time point. The second criterion was set as either no change or increase in the maximum standardized uptake value between the two time points. Sensitivity, specificity and accuracy were calculated for the three methods by using the biopsy results and clinical follow up as gold standard.

**Results:** Biopsy and follow-up revealed 72 patients with malignant lung nodules, whereas 193 patients had benign nodules. Single time point imaging with a threshold maximum standardized uptake value of 2.5 had a sensitivity, specificity and accuracy of 63%, 92% and 85% respectively. On dual-time-point imaging, for the initial criterion for malignancy, the sensitivity, specificity and accuracy were 81%, 95% and 91% respectively. On dual time point imaging, for the second criterion for malignancy, the sensitivity, specificity and accuracy were 92%, 93%, and 92% respectively.

**Conclusion:** Dual-time-point FDG PET imaging using both criteria has higher sensitivity, specificity and accuracy compared to single time imaging. Dual-time-point FDG PET imaging should be included in the clinical workup of patients with pulmonary nodule.

**Key Words:** Dual-time-point imaging, FDG-PET, Solitary pulmonary nodule

**JRMS August 2008; 15(2): 6-14**

---

From the Department of Radiology, Nuclear Medicine Division,

\*King Hussein Medical Center, (KHMC), Amman-Jordan

\*\*Hospital of the University of Pennsylvania, Philadelphia, PA, USA

Corresponding should be addressed to Dr. K. Alkhaldeh, (KHMC), E-mail: [khaledk73@gmail.com](mailto:khaledk73@gmail.com).

Manuscript received June 3, 2007. Accepted November 15, 2007

## Introduction

Solitary pulmonary nodules are defined as focal, round or oval areas of increased opacity in the lung that measure less than three cm in diameter.<sup>(1,2,3)</sup> An estimated 150,000 solitary pulmonary nodules are detected annually in the United States and are often discovered incidentally at chest radiography or computed tomography (CT).<sup>(3,4)</sup> These nodules are caused by a variety of disorders including neoplasms, infection, inflammation, and vascular and congenital abnormalities. Although most solitary pulmonary nodules have benign causes, 30%–40% of these nodules are malignant.<sup>(4-6)</sup>

<sup>18</sup>F-FDG has established role in oncology, which includes initial diagnosis, staging, and therapeutic follow-up studies.<sup>(7,8)</sup> Despite its proven utility, the application of PET is limited by its variable sensitivity and specificity estimates. One of the main reasons for this limitation is that many inflammatory lesions also have elevated <sup>18</sup>F-FDG uptake in PET, leading to false-positive results.<sup>(9,10)</sup> On the other hand, some types of cancers, for example, carcinoid tumor and bronchoalveolar carcinomas, have low <sup>18</sup>F-FDG uptake below the diagnostic threshold for <sup>18</sup>F-FDG uptake in malignant lesions.<sup>(11,12)</sup>

A maximum standardized uptake value (SUV) of 2.5 as a cutoff criterion for malignancy has been used for diagnosing pulmonary malignancies with <sup>18</sup>F-FDG PET.<sup>(13-20)</sup> However, one study indicated that the sensitivity of this SUV cutoff was lower than that of visual assessment.<sup>(21)</sup> Some authors have recommended using visual evaluation rather than the SUV for small solitary pulmonary nodules,<sup>(22)</sup> suggesting that the classical SUV criterion of 2.5 is inappropriate for diagnosing malignancies with low <sup>18</sup>F-FDG uptake.<sup>(21,23)</sup> Studies have shown that the uptake of <sup>18</sup>F-FDG continues to increase in malignant tumors for several hours after <sup>18</sup>F-FDG injection.<sup>(10,12)</sup> It has been deduced that this difference in the time course of <sup>18</sup>F-FDG uptake could be used to improve the ability of PET to distinguish benign lesions from malignant lesions. Preliminary studies have been performed using FDG PET with dual-time-point imaging on head and neck cancers, breast cancer and malignant lung lesions. Those results demonstrated significant improvement in the diagnostic accuracy of FDG PET scan.<sup>(12,21-25)</sup>

On the basis of the promising results from dual-time-point imaging research, the present study was undertaken to assess whether dual-time-point

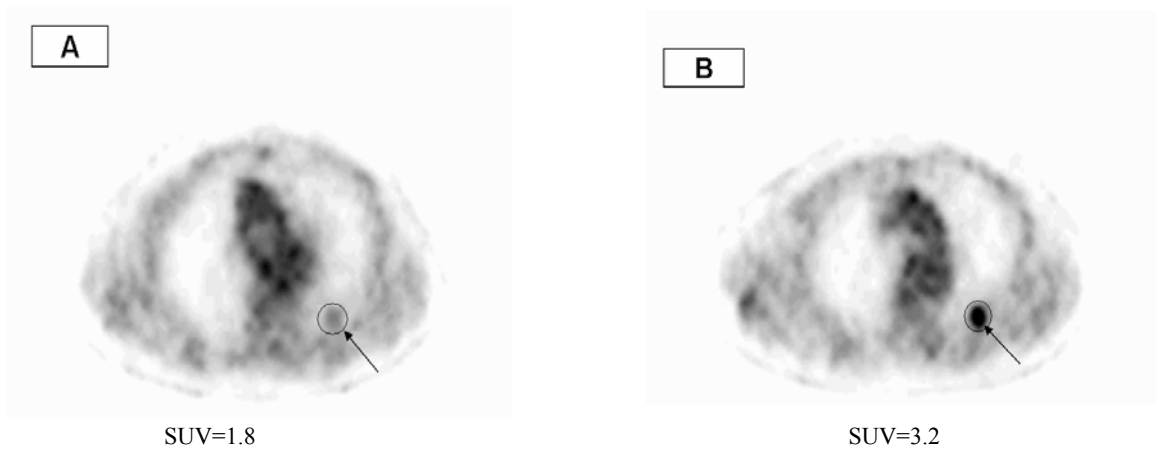
acquisition can improve the diagnostic utility of PET in Solitary Pulmonary nodules.

## Methods

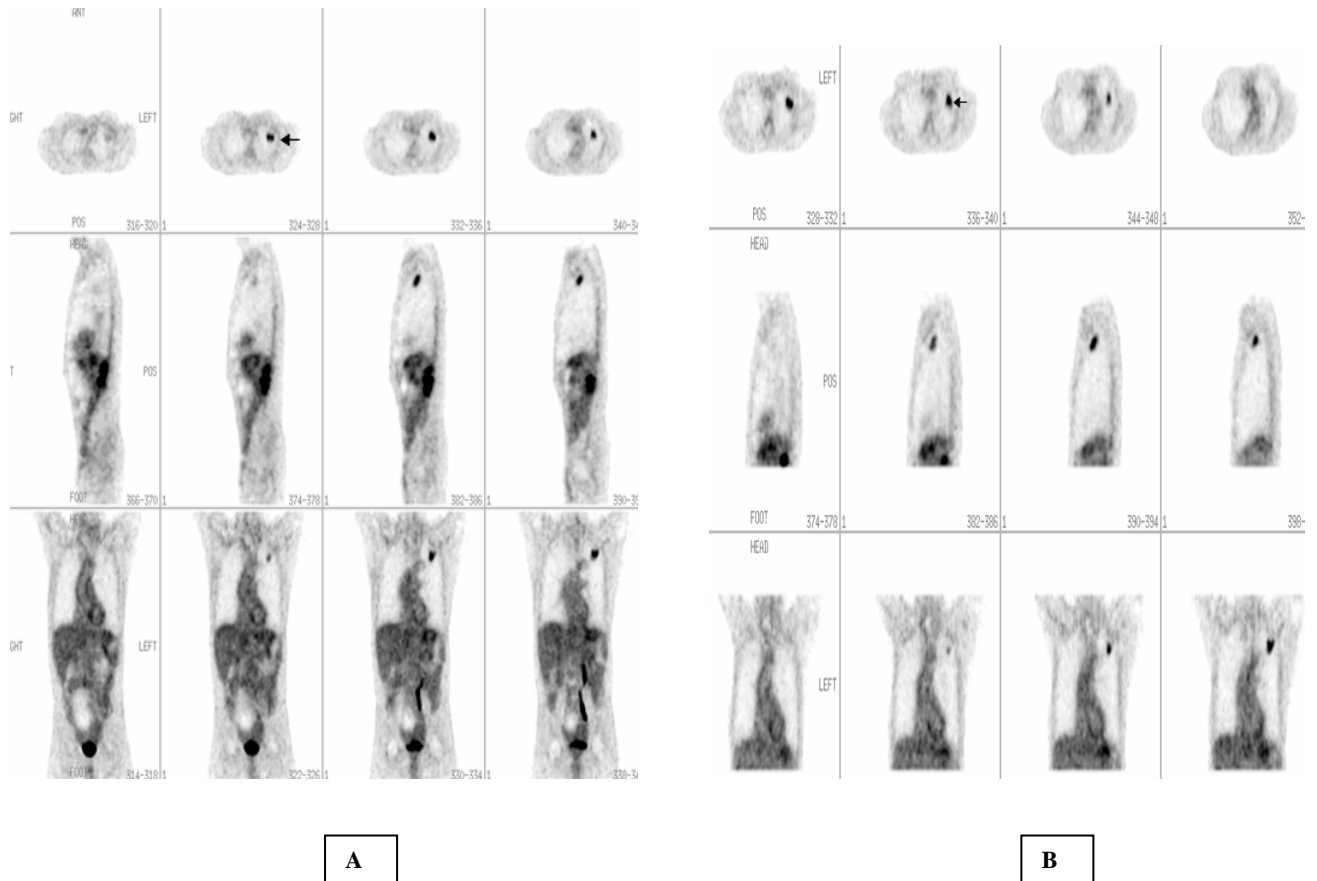
This retrospective study was conducted in the Hospital of the University of Pennsylvania, and data was collected and analyzed in the period from September 2005 to March 2006, from the pooled hospital studies for the last five years. Two hundred sixty five patients (161 men, 104 women; mean age 67 years; age range: 41–92 years) were included in this retrospective analysis. All patients had suspected solitary pulmonary nodules detected by CT. All our study patients had <sup>18</sup>F-FDG PET and CT scanning acquired in two different occasions, with a time gap (0-35 days). All patients underwent whole body PET scans, and 255 patients were examined twice: initial whole-body imaging followed by a second scan for the chest only. Informed consent was obtained from all patients. At the time of <sup>18</sup>F-FDG injection all patients had fasted for at least four hours and had blood sugar levels of <150 mg/dL.

Image acquisition for the whole-body scan started at a mean time point of 60 minutes after injection of 2.52 MBq/kg of body weight. This first scan (scan A) included neck, thorax, abdomen, pelvis and upper thighs. It consisted of four or five emission frames of 25.6-cm length with an overlap of 12.8 cm covering an axial length of 64–76.8 cm, including six to seven beds and duration of the scan was 18-21 minutes. A second emission scan of the thorax only (scan B) was acquired on 255 patients at a mean time of 110 minutes after tracer injection (range 100–120 min), including two beds and duration of scan was ranging between six minutes. A transmission scan was obtained with both sets of images for attenuation correction. Image reconstruction was performed with an iterative ordered-subsets expectation maximization algorithm with four iterations and eight subsets. Attenuation-corrected images were obtained by applying transmission maps, which were acquired after <sup>18</sup>F-FDG injection with a <sup>137</sup>Cs source interleaved with the emissions scans.

Regions of interest (ROIs) were overlaid onto the lesions on fully corrected PET images of scans A and B axial slices (Fig. 1). This was achieved by direct visual assessment of the lesion position on the CT scan and subsequent identification of the corresponding area on PET scans A and B.



**Fig.1.** An axial slices region of interest (ROI) were placed around the lesion on first time (A) and second time (B) images, in order to calculate the maximum SUV



**Fig. 2.** Dual-time-point FDG PET imaging of 60 years old man with 1.8 cm solitary pulmonary nodule in the left lung on transverse, sagittal and axial slices. First time whole body image (A) shows a focal area with FDG upatke (arrow) and with SUV= 2.5. Second time image of the chest(B) shows more prominent FDG upatke with SUV=2.9. Pathological diagnosis of this nodule was moderately differentiated adenocarcinoma

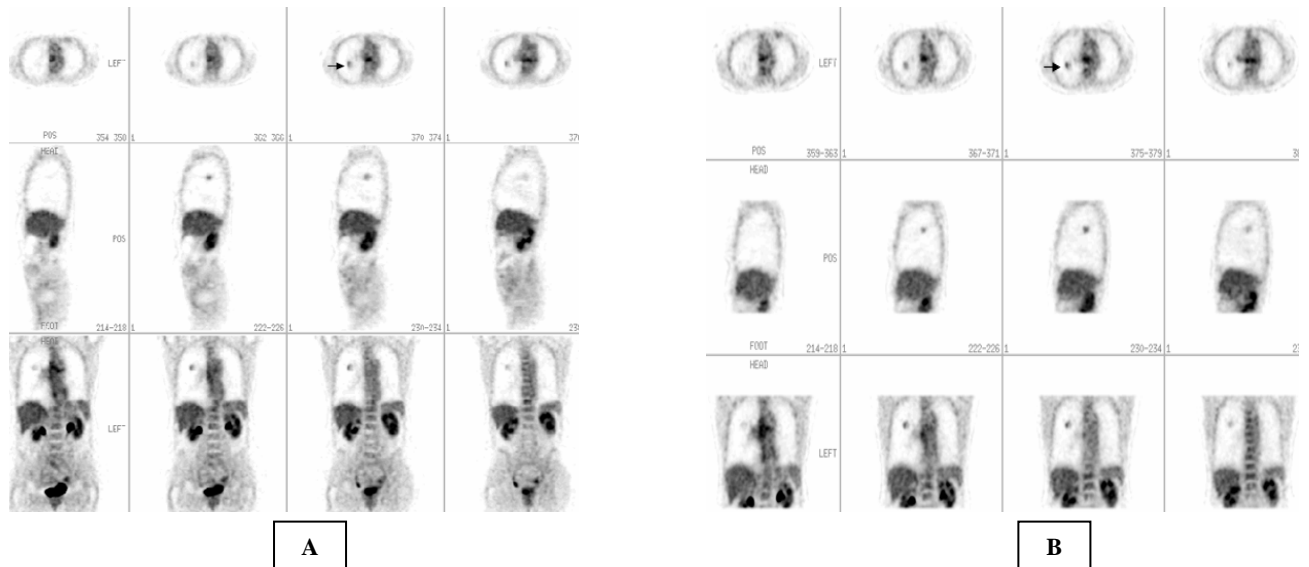


**Fig. 3.** Dual-time-point FDG PET imaging of 65 years old male patient with 1.4cm pulmonary nodule in the right lung on transverse, sagittal and axial slices . First time whole body image (A) shows an area with FDG uptake ( arrow), with SUV= 1.8 and second time image of the chest(B) with SUV =2.3. Pathological diagnosis of this nodule was bronchioloalveolar adenocarcinoma

In tumor lesions that extended over several slices in the craniocaudal direction, the ROI was placed in the midportion of the lesion where the maximal SUV was measured. If no discernible uptake was present on either PET scan, ROIs were drawn in the presumed location that corresponded best with that of the radiographic density. The maximum Standardized uptake value (SUV) of the lung lesions were calculated from scan A and scan B according to the following standard formula: Mean ROI activity (MBq/g) / [Injected dose (MBq)/ Body weight (g)].

We used three criteria in the assessment of pulmonary nodules; first criterion is the classical single time imaging using SUV of 2.5 as cut off criterion for malignancy. We adopted two criteria on dual time point imaging; first criterion was set as any increase in SUV between the first and second scans as a criterion for malignancy, while second criterion was set as any increase or no change in SUV between the first and second scan as criterion for malignancy. All nodules with no FDG uptake that had SUV=lung background activity were considered as negative for malignancy in all criteria.

Benign or malignant diagnosis of the nodules was established using biopsy or clinical follow up data. The sensitivity, specificity, accuracy, negative predictive value (NPV) and positive predictive values (PPV) for the three criteria were calculated.

## Results

Of the 265 nodules included in this study, 72 (27%) proved to be malignant and 193 (73%) benign. The sizes of these 265 nodules were as follows: 32 nodules <1 cm in diameter, 57 nodules 1-1.5 cm and 176 nodules 1.6-3 cm. Diagnoses of 158 nodules were decided to be benign according to the clinical follow up data.

On single time point imaging, 60 nodules had  $SUV \geq 2.5$  (45 malignant and 15 benign), 205 nodules had  $SUV < 2.5$  (27 malignant and 178 benign). While 119/205 nodules did not show any visually apparent FDG uptake in the first scan and SUVs of those lesions were equal to the lung background.

On dual-time-point imaging, 60 nodules had increased in SUV between scan A and scan B (50 malignant and 10 benign), 70 nodules had drop in SUV (three malignant and 67 benign) and 11 nodules had no change in SUV (seven malignant and four benign). One hundred and fourteen nodules had no FDG uptake on scan A and B and the calculated  $SUV = \text{lung background}$  (two malignant and 112 benign). Figures 2 & 3 show dual-time-point imaging in two patients with malignant pulmonary nodules, including SUV change and histopathology diagnosis.

When assessing the diagnostic value of the first emission scan by applying an SUV threshold of 2.5

for separating benign from malignant lesions, sensitivity, specificity and accuracy were 63%, 92% and 84% respectively. When applying this criterion to small nodules of less than 1cm, the values were 50%, 90% and 75% respectively compared to 65%, 93% and 85% for larger nodules.

When any increase in SUV between the first and second scans was applied as a criterion for malignancy, the sensitivity, specificity and accuracy were 83%, 95% and 91% respectively. When any increase or no change in SUV between the first and second scans criterion was applied, the values were 92%, 93%, and 92% respectively. Table I and II shows SUV1, SUV2 and histopathological diagnoses for benign and malignant lung nodules. Table III shows the sensitivity, specificity, accuracy, NPV and PPV in the three criteria used in our study according to single time SUV and dual time change.

## Discussion

In addition to visual assessment of the metabolic activity of the nodules, measurement of the SUV for the semiquantitative assessment of  $^{18}\text{F}$ -FDG uptake in pulmonary lesions has proven to assist in differentiating between malignant and benign nodules.<sup>(13-20)</sup> Several reports consider it to be a simple and useful tool for this purpose, and most publications conclude that a threshold value of 2.5 is optimal for obtaining a high sensitivity while maintaining a good specificity.<sup>(13-20)</sup> However, several reports and observations on the day-to-day clinical practice indicate that a significant degree of overlap exists between the uptake values of benign and malignant lesions.<sup>(16-18)</sup> Certain inflammatory lesions, including granulomatous processes, fungal infections, or bacterial infections, can be noted with SUVs of  $>2.5$ ,<sup>(15,26)</sup> thereby limiting specificity of this method. Most inflammatory lesions would fall below the 2.5 SUV thresholds, whereas the majority of malignant lesions would have high SUVs. However, small malignant lesions may have under

estimated SUV due to partial volume effect and limited resolution of PET scanner.<sup>(27-28)</sup> On the other hand, carcinoid tumor and bronchoalveolar carcinomas can have low levels of  $^{18}\text{F}$ -FDG uptake, and the SUV in such tumors may fall below the 2.5 limit for malignancy in this criterion.<sup>(11,12)</sup> Those factors have potential effect on the diagnostic accuracy of using this criterion, because it can lead to misinterpretation of malignant lesions into benign ones.

In our study, when adopting the  $\text{SUV} \geq 2.5$  as criterion for malignancy, the sensitivity, specificity and accuracy were 63%, 92% and 84% respectively. Our results have lower sensitivity and comparable specificity compared to those published in the literature.<sup>(13-18)</sup> When applying this criterion to small nodules of less than 1cm, the values were 50%, 90% and 75% compared to 65%, 93% and 85% for larger nodules. This can show the limitation of this criterion induced primarily by underestimation of SUV due to impact of partial volume effect.

Dual-time-point FDG PET imaging was suggested as discriminator of benign and malignant diseases, with images being obtained at one and two hours after the administration of  $^{18}\text{F}$ -FDG. Hustinx *et al.*<sup>(9)</sup> had acquired dual time point imaging for head and neck tumors, and he used a threshold of 10% increase in measured values. He reported higher sensitivity (100% vs. 80%), while maintaining an excellent specificity (89% vs. 94%), than that obtained from a single image acquisition using the usual SUV threshold method. Zhuang *et al.*<sup>(10)</sup> found that malignant lesions showed a significant increase in SUV over time and that benign lesions showed a decrease over time. Lodge *et al.*<sup>(26)</sup> came to a similar conclusion in a study of 29 patients with various benign and malignant soft-tissue masses. Rakesh *et al.*<sup>(25)</sup> had applied dual time point imaging in breast cancer, and found that breast malignancies show increasing FDG uptake with time, whereas the uptake of  $^{18}\text{F}$ -FDG in inflammatory lesions and normal breast tissues decreases over time.

**Table I.** SUV1 and SUV2 in malignant lung nodules

SUV1	SUV2	Final diagnosis	SUV1	SUV2	Final diagnosis
2.5	2.6	Poorly differentiated adenocarcinoma	2.1	2.3	Bronchioloalveolar adenocarcinoma
1	1.6	Differentiated adenocarcinoma	4.2	4.8	Lung adenocarcinoma of moderately differentiated,
1.7	2.4	Metastatic adenocarcinoma of breast	2.5	2.8	Well-differentiated pulmonary adenocarcinoma
2.9	4	Poorly differentiated adenocarcinoma	2.7	3	Moderately differentiated adenocarcinoma
7.5	10	Squamous cell carcinoma	1.3	1.5	Poorly differentiated adenocarcinoma
3.1	4.1	moderately differentiated adenocarcinoma	5.8	6.5	Poorly differentiated adenocarcinoma
3.1	4.1	Small cell lung cancer	1.6	1.8	Mucinous adenocarcinoma Colon metastasis
1	1.3	Moderately differentiated adenocarcinoma	4.3	4.8	Adenocarcinoma, moderately differentiated
3.1	4	Poorly differentiated adenocarcinoma	2	2.3	Poorly differentiated adenocarcinoma
1.8	2.3	Carcinoma of neuroendocrine origin, possible small cell lung cancer	4.8	5.4	Metastatic esophageal adenocarcinoma
2.9	3.7	Poorly differentiated adenocarcinoma	2.7	3	Well diff. adenocarcinoma
5.9	7.5	Well-differentiated adenocarcinoma	6.1	6.4	Well-differentiated adenocarcinoma
4.6	5.8	Bronchioloalveolar adenocarcinoma	6	6.5	Poorly differentiated adenocarcinoma,
5.4	6.8	Squamous cell lung cancer	17.7	17.7	Moderately differentiated adenocarcinoma
2.8	3.5	Metastatic transitional cell ca of bladder	5.4	5.4	Moderately differentiated adenocarcinoma
1.2	1.5	Moderate-poor differentiated Squamous cell carcinoma	3.4	3.4	Moderately differentiated adenocarcinoma
1.2	1.5	Moderately differentiated adenocarcinoma	2.2	2.2	Differentiated adenocarcinoma
1.8	2.2	Well differentiated adenocarcinoma	2.3	2.3	Bronchioloalveolar adenocarcinoma
7.4	9	Squamous cell lung cancer	2	2	Metastatic melanoma
4.7	5.7	Poorly differentiated adenocarcinoma	1.7	1.7	Bronchoalveolar adenocarcinoma
2.1	2.5	Poorly differentiated adenocarcinoma	2.6	2.5	Metastatic germ cell tumor
2.1	2.5	Poorly differentiated adenocarcinoma	2.8	2.6	Metastatic breast cancer
1.1	1.3	Moderately differentiated adenocarcinoma	2.8	2.6	Atypical carcinoid
1.2	1.4	Moderately differentiated adenocarcinoma	1.4	1.3	Carcinoid
2.6	3	Adenocarcinoma	2.5	2.3	Adnocarcinoma
1.3	1.5	Bronchioloalveolar adenocarcinoma	0.5	0.7	carcinoid
3.3	3.8	Poorly differentiated adeno carcinoma	15		Poorly differentiated adenocarcinoma
2.7	3.1	Poorly differentiated non-small cell carcinoma	13.7		Metastatic vocal cord tumor
2.7	3.1	Poorly differentiated Adenocarcinoma	10.6		Poorly differentiated squamous cell carcinoma
2.7	3.1	Metastatic transitional cell carcinoma	7.7		Non Small cell cancer, Large cell cancer
7	8	Poorly differentiated adenocarcinoma, with focal sarcomatoid features	4.4		Bronchioloalveolar adenocarcinoma
2.3	2.6	Moderately differentiated adenocarcinoma	3.4		Poorly differentiated adenocarcinoma
1.7	1.9	Mucinous adenocarcinoma metastasis of colon	3		Baldder adenocarcinoma mets
1.8	2	Bronchioalveolar adenocarcinoma	2.9		Moderately differentiated adenocarcinoma
2	2.2	Carcinoid	2.8		Moderate to poorly differentiated adenocarcinoma
2	2.2	Small cell cancer	2.5		Metastatic melanoma

**Table II.** SUV1 and SUV2 in benign lung nodules

SUV1	SUV2	Final diagnosis	SUV1	SUV2	Final diagnosis
2.6	2.8	Sarcoidosis	2.3	2.1	Decreased in size by CT
3.5	4.1	Inflammation	1.9	1.4	Inflammation
2.6	2.3	Granuloma	1.6	1.2	decreased size by CT
2.7	2.1	Inflammatory	1.6	1.2	Granuloma
2.9	2.5	Mycobacterium Infection	2.5	2.1	Inflammation
3.2	1.6	Inflammation	1.4	1.3	Stable on F/U CT
2.5	2.1	Inflammation	2.3	2.4	Histoplasmosis with granuloma
2.6	2.7	Chondromatous hamartomas	2	1.6	Inflammation
2.8	2.4	Stable on CT	2.3	1.9	Stable
2.6	2.6	Resolved on CT	1.5	1.6	Inflammation
2.7	2.2	Inflammation	2.1	1.6	Stable
2.8	2.4	Fibrosis	1.8	2.4	Apical sub pleural fibrosis
2.6	2.6	Inflammation	2	1.8	Resolved on CT
2.5	2.2	Stable in PET F/U	2.1	1.7	Inflammation
2.6	2.3	Stable on CT F/U	2.2	2	Inflammation
1.2	1.2	Inflammation	1.4	1.1	Stable on CT
2.2	1.8	Resolved CT	2.2	1.9	Noncaseating Granuloma
2.1	2.1	Chronic inflammation	2.1	2	Stable on CT
1.4	1.4	Stable on CT	1.8	1.6	Inflammation
2	1.7	Fibrosis	2.4	2.6	Granuloma
1.9	1.5	Resolved on CT	1.7	3.5	Inflammation
1.9	1.6	Inflammation	1.9	1.8	Stable
2.3	2.8	Inflammatory	2.4	2.5	Atypical Mycobacterial Infection
1.7	1.6	Stable in CT	1.1	0.9	Decreased size
2.3	2.1	Inflammation	1.8	1.5	Granuloma
1.4	2.1	Granuloma	2.4	2.2	Inflammation
1.9	1.7	Hamartomas			

**Table III.** The results of statistical analysis in three different methods used in the assessment of solitary pulmonary nodules

Criteria	FN	FP	TP	TN	Sensitivity	Specificity	Accuracy	PPV	NPV
SUV $\geq$ 2.5	27	15	45	178	63%	92%	84 %	71%	89%
Any increase in SUV on Dual-time-point imaging	12	10	50	183	83%	95%	91%	83%	94%
Increase or no change in SUV on Dual-time-point imaging	5	14	57	179	92%	93%	92%	78%	97%

Hamberg *et al.*<sup>(29)</sup> showed that the usual scan start times of 45–60min lead to significant underestimation of the true SUV because, in most tumors, <sup>18</sup>F-FDG uptake continues to rise beyond this period and typically does not reach a plateau for several hours. In untreated tumors, 95% of the plateau value was reached at  $298 \pm 42$  min, with a range of 130–500 min.

We set two criteria for the assessment of pulmonary nodules with dual-time-point imaging, in order to decide which is going to give us the most accurate results when compared to biopsy and clinical follow up. In our first criterion with any increase in SUV between the first and second scans had sensitivity, specificity and accuracy of 83%, 95% and 91% respectively vs. 63%, 92% and 84%

for single time point imaging with SUV  $\geq$  2.5 criterion. This criterion shows clear benefit of dual time point imaging in improving the sensitivity while maintaining good specificity. When the criterion was changed into any increase or no change between the two scans, sensitivity, specificity and accuracy were 92%, 93% and 92% respectively. In this criterion there were seven malignant nodules which did not show any change in SUV on dual-time-point imaging, and the interpretation of which was changed from false negative into true positive. The sensitivity of PET increased to 92% when the second dual-time-point criterion was used vs. 63% in single-time-point PET. On the other hand, dual-time-point imaging using the later criterion has a high negative

predictive value for malignant nodule (97%). This high negative predictive value may allow us to wait and have a follow-up evaluation of the SPN after a certain time interval of three or six months.

Matthies *et al.*<sup>(12)</sup> compared single-time-point imaging and dual-time-point imaging with a cutoff SUV of 2.5 and a 10% increase in SUV for malignancy in 36 pulmonary nodules, which was a relatively small study group; the authors determined that the sensitivity and specificity of the tests were 80% and 94% (single) and 100% and 89% (dual), respectively. Although there is clear benefit of dual-time-point imaging using this criterion, still in our study there were 10 malignant lesions that did not reach the 10% increase in SUV (drop in three and no change in seven), and this criterion can result in misinterpretation of those lesions as benign.

Our results are in contrast to a study by Lowe *et al.*<sup>(18)</sup> who assessed the change in SUV over time in a cohort of 14 patients with pulmonary abnormalities (10 malignant, four benign). On the basis of measurement of the signal-to-noise ratio, the best separation between benign and malignant lesions occurred at 50 minutes after injection and no improvement was seen at later time points.

This study included 57 FDG avid benign lung nodules. Pathological diagnosis of FDG avid benign lesions that had increase or no change in SUV included: inflammation, granuloma, histoplasmosis, mycobacterial infection, and sarcoidosis. Also in the literature some benign granulomatous lesions, such as sarcoidosis, aspergillosis, and coccidiomycosis, have been reported to be <sup>18</sup>F-FDG avid and to show increasing uptake over time and producing false positive results.<sup>(20,30,31)</sup>

The limitation in the present study is that during semiquantitative analysis with only a PET scanner, the ROI location that corresponded to the lesion site was difficult to determine only on PET images when the lesion was faint or presence of other FDG avid benign lesions. Thus, we selected a nearby location by using corresponding CT slices; this method would have produced some inaccuracies in SUV measurements. This problem can be resolved by using a PET/CT scanner, because the ROI location can be determined easily by use of fused PET and CT images. However, the use of dual-time-point imaging would add to diagnostic accuracy, especially for small lesions that have lower SUVs, and in differentiating inflammation from malignant

lesions; this increase in diagnostic accuracy would compensate for the extended length of each scan.

## Conclusion

Dual time point FDG Positron Emission Tomography using both criteria has higher sensitivity, specificity and accuracy compared to single time imaging. Dual time point FDG Positron Emission Tomography should be included in the clinical workup of patients with solitary pulmonary nodule.

## References

1. **Ost D, Fein A, Feinsilver S.** Clinical practice. The solitary pulmonary nodule. *N Engl J Med* 2003; 348(25): 2535-2542.
2. **Chin Y, Kyung L, Byung-Tae K, et al.** Tissue Characterization of Solitary Pulmonary Nodule: Comparative Study Between Helical Dynamic CT and Integrated PET/CT. *J Nucl Med* 2006; 47: 443-450.
3. **Leef J, Klein I.** The solitary pulmonary nodule. *Radiol Clin North Am* 2002; 40: 123-143.
4. **Tan B, Flaherty K, Kazerooni E, et al.** The Solitary Pulmonary Nodule. *Chest.* 2003; 123: S89-S96.
5. **Gurney J.** Determining the likelihood of malignancy in solitary pulmonary nodules with Bayesian analysis. Part I. Theory. *Radiology* 1993; 186: 405-413.
6. **Patz E.** Evaluation of Focal Pulmonary Abnormalities with FDG PET. *Radiographics* 2000; 20: 1182-1185.
7. **Rohren E, Turkington T, Coleman R.** Clinical applications of PET in oncology. *Radiology* 2004; 231: 305-332.
8. **Kumar R, Bhargava P, Bozkurt M, et al.** Positron emission tomography imaging in evaluation of cancer patients. *Indian J Cancer* 2003; 40: 87-100.
9. **Hustinx R, Smith RJ, Benard F, et al.** Dual time point fluorine-18 fluorodeoxyglucose positron emission tomography: a potential method to differentiate malignancy from inflammation and normal tissue in the head and neck. *Eur J Nucl Med* 1999; 26: 1345-1348.
10. **Zhuang H, Pourdehnad M, Lambright ES, et al.** Dual time point <sup>18</sup>F-FDG PET imaging for differentiating malignant from inflammatory processes. *J Nucl Med* 2001; 42: 1412-1417.
11. **Buck A, Schirrmester H, Kuhn T, et al.** FDG uptake in breast cancer: correlation with biological and clinical prognostic parameters. *Eur J Nucl Med Mol Imaging* 2002; 29: 1317-1323.

12. **Matthies A, Hickeson M, Cuchiara A, et al.** Dual-time-point <sup>18</sup>F-FDG PET for the evaluation of pulmonary nodules. *J Nucl Med* 2002; 43: 871–875.
13. **Al-Sugair A, Coleman R.** Applications of PET in lung cancer. *Semin Nucl Med* 1998; 28: 303–319.
14. **Kubota K, Matsuzawa T, Fujiwara T, et al.** Differential diagnosis of lung tumor with positron emission tomography: a prospective study. *J Nucl Med* 1990; 31: 1927–1932.
15. **Gupta N, Frank A, Dewan N, et al.** Solitary pulmonary nodules: detection of malignancy with PET with 2-[F-18]-fluoro-2-deoxy-D-glucose. *Radiology* 1992; 184: 441–444.
16. **Patz E, Lowe V, Hoffman J, et al.** Focal pulmonary abnormalities: evaluation with F-18 fluorodeoxyglucose PET scanning. *Radiology* 1993; 188: 487–490.
17. **Dewan N, Gupta N, Redepenning L, et al.** Diagnostic efficacy of FDG-PET imaging in solitary pulmonary nodules: potential role in evaluation and management. *Chest* 1993; 104: 997–1002.
18. **Lowe V, Fletcher J, Gobar L, et al.** Prospective investigation of positron emission tomography in lung nodules. *J Clin Oncol* 1998; 16: 1075–1084.
19. **Präuer H, Weber W, Römer W, et al.** Controlled prospective study of positron emission tomography using the glucose analogue [<sup>18</sup>F] fluorodeoxyglucose in the evaluation of pulmonary nodules. *Br J Surg* 1998; 85: 1506–1511.
20. **Kotaro H, Yoshimichi U, Hiroyasu S, et al.** Fluorine-18-FDG PET imaging is negative in bronchioalveolar carcinoma. *J Nucl Med* 1998; 39: 1016–1020.
21. **Nomori H, Watanabe K, Ohtsuka T, et al.** Visual and semiquantitative analyses for F-18 fluorodeoxyglucose PET scanning in pulmonary nodules 1 cm to 3 cm in size. *Ann Thorac Surg* 2005; 79: 984–988.
22. **Herder G, Golding R, Hoekstra O, et al.** The performance of <sup>18</sup>F-fluorodeoxyglucose positron emission tomography in small solitary pulmonary nodules. *Eur J Nucl Med Mol Imaging* 2004; 31: 1231–1236.
23. **Yaichiro H, Tetsuya T, Chisato K, et al.** Accuracy of PET for Diagnosis of Solid Pulmonary Lesions with <sup>18</sup>F-FDG Uptake below the Standardized Uptake Value of 2.5. *Journal of Nuclear Medicine* 2006; 47(3): 426–431
24. **Demura Y, Tsuchida T, Ishizaki T, et al.** <sup>18</sup>F-FDG accumulation with PET for differentiation between benign and malignant lesions in the thorax. *J Nucl Med* 2003; 44: 540–548.
25. **Kumar R, Loving V, Chauhan A, et al.** Potential of Dual-Time-Point Imaging to Improve Breast Cancer Diagnosis with <sup>18</sup>F-FDG PET. *J Nucl Med* 2005; 46: 1819–1824.
26. **Lodge M, Lucas J, Marsden P, et al.** A PET study of <sup>18</sup>FDG uptake in soft tissue masses. *Eur J Nucl Med* 1999; 26: 22–30.
27. **Hickeson M, Yun M, Matthies A, et al.** Use of a corrected standardized uptake value based on the lesion size on CT permits accurate characterization of lung nodules on FDG-PET. *Eur J Nucl Med Mol Imaging* 2002; 29: 1639–1647.
28. **Dewan N, Shehan C, Reeb S, et al.** Likelihood of malignancy in a solitary pulmonary nodule: comparison of Bayesian analysis and results of FDG-PET scan. *Chest* 1997; 112: 416–422.
29. **Hamberg L, Hunter G, Alpert N, et al.** The dose uptake ratio as an index of glucose metabolism: useful parameter or oversimplification? *J Nucl Med* 1994; 35: 1308–1312.
30. **Knight S, Delbeke D, Stewart J, et al.** Evaluation of pulmonary lesions with FDG-PET. *Chest* 1996; 109: 982–988.
31. **Kapucu L, Meltzer C, Townsend D, et al.** Fluorine -18- fluoro- deoxyglucose uptake in pneumonia. *J Nucl Med* 1998; 39: 1267–1269.